Hyperconjugative Effects on π^* Negative Ion States. Electron Transmission Spectroscopy of Cycloalkenes

Stuart W. Staley,*[1a,b] Allison E. Howard,[1b] and Jeffrey T. Strnad[1a]

Departments of Chemistry, Carnegie Mellon University, Pittsburgh, Pennsylvania 15213, and University of Nebraska—Lincoln, Lincoln, Nebraska 68588

Received August 5, 1991

The vertical electron attachment energies (AEs) for the π^* negative ion states of the C_3–C_8 *cis*-cycloalkenes have been determined by electron transmission spectroscopy. AE increases on going from cyclopropene to cyclopentene and cyclohexene, then decreases for cycloheptene and increases for *cis*-cyclooctene. Geometry-optimized structures have been calculated for all compounds at the HF/6-31G level of ab initio molecular orbital theory. AE values have been analyzed on the basis of both Koopmans' theorem and the differences in total energies of the ground and negative ion states at the HF/6-31G*//HF/6-31G level. Almost all of the variation in AE(π^*) can be ascribed to hyperconjugation effects. The latter have been evaluated in terms of the π-electron density of the double bond, the values of key C,H overlap integrals, and the basis orbital energies of the alkyl bridge. As a general result, AE(π^*) tends to be at a maximum when the allylic substituents are staggered with respect to the alkene hydrogen owing to the overlap of σ_π^* with π^* being at a maximum. The structural origin of each of these factors is discussed.

In this paper we address the general problem of how molecular conformation influences the energetic contribution of hyperconjugation in π^* negative ion states. Previous workers have considered this question with respect to various neutral and charged species,[2] but little has been published with respect to unbound negative ion states.[3] This is an especially interesting problem because of the highly diffuse nature of these states and the consequent possibility of significant long-range interactions.

We have determined electron attachment energies (AEs) associated with the π^* orbitals in cycloalkenes by the technique of electron transmission spectroscopy (ETS).[4] The AEs are normally taken to be the negative of the vertical electron affinities and, by the use of Koopmans' approximation,[5] can be correlated with the corresponding π^* orbital energies calculated by molecular orbital theory. The latter correlation holds with varying degrees of success for various classes of compounds,[6,7a] but is valid for alkenes and polyenes.[7]

The C_3 through C_8 *cis*-cycloalkenes (**3**–**8**) represent a fundamental series of molecules, the π^* AEs of all members of which have been measured by at least one group. The data currently in the literature indicate that AE(π^*) increases from 1.73 eV for cyclopropene (**3**)[7a] to as high as 2.26 eV for cyclopentene (**5**)[8] and then decreases to 1.97 and 1.87 eV for cycloheptene (**7**) and cyclooctene (**8**), respectively.[8]

We have previously explained the AE of **3** relative to ethylene (**1**) on the basis of two offsetting effects. AE of

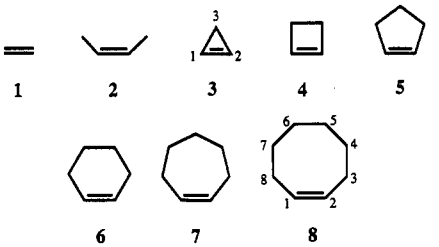

3 is increased owing to a shorter (by 0.04 Å) double bond but is decreased by hyperconjugative donation of electron density from π to the pseudo-π^* orbital at C_3 (σ_π^*), thus reducing the screening of π^* by the π electrons.[7a] The greater AEs of *cis*-2-butene (**2**)[7a] and **4**–**6** can be rationalized on the basis of hyperconjugation with the adjacent CH_2 groups, but the smaller increase for **4** relative to **2**, **5**, and **6** has not been satisfactorily explained.

Finally, the stabilization of π^* on going from **5** to **8** has been attributed to the increased importance of mixing with pseudo-π^* orbitals in the larger alkyl groups.[8] In this study, we present a revision of the experimental ordering of the AEs of several of the *cis*-cycloalkenes along with theoretical calculations that permit a detailed understanding of the smaller AEs of **4**, **7**, and **8** relative to **5** and **6**. Our data provide new insights concerning the role of hyperconjugation in π^* negative ion states.

Experimental Section

Materials. *Cyclopropene* was synthesized by the method of Closs and Krantz[9] and purified by trap-to-trap distillation. *Cyclobutene* was prepared by the method of Cope et al.[10] and purified by bubbling through molten maleic anhydride.[11] All other compounds were obtained from Aldrich Chemical Co.

Electron Transmission Spectroscopy. The technique of ETS involves passing a monoenergetic beam of electrons through a static sample in the gas phase.[4] At certain energies a decrease in the transmitted current is observed owing to electron scattering that originates from temporary (ca. 10^{-14} s) capture of electrons by sample molecules. The actual scattering events, as well as the corresponding variations in the ET spectra (Figure 1), are termed "resonances". The energy of a resonance (or negative ion state) is termed the electron attachment energy (AE).

After passing through the collision chamber, the electrons enter a retarding region where a variable potential prevents a portion

(1) Address correspondence to (a) Carnegie Mellon University; (b) University of Nebraska—Lincoln.

(2) Review: Radom, L. *Prog. Theor. Org. Chem.* **1982**, *3*, 1.

(3) (a) Staley, S. W.; Giordan, J. C.; Moore, J. H. *J. Am. Chem. Soc.* **1981**, *103*, 3638. (b) Balaji, V.; Ng, L.; Jordan, K. D.; Paddon-Row, M. N.; Patney, H. K. *J. Am. Chem. Soc.* **1987**, *109*, 6957.

(4) (a) Sanche, L.; Schulz, G. J. *Phys. Rev. A* **1972**, *5*, 1672. (b) Schultz, G. J. *Rev. Mod. Phys.* **1973**, *45*, 378, 423. (c) Jordan, K. D.; Burrow, P. D. *Chem. Rev.* **1987**, *87*, 557. (d) Allan, M. *J. Electron Spectrosc. Relat. Phenom.* **1989**, *48*, 219.

(5) Koopmans, T. *Physica* **1934**, *1*, 104.

(6) (a) Younkin, J. M., Smith, L. J.; Compton, R. N. *Theor. Chim. Acta* **1976**, *41*, 157. (b) Dewar, M. J. S.; Rzepa, H. S. *J. Am. Chem. Soc.* **1978**, *100*, 784. (c) Kreile, J.; Schweig, A.; Thiel, W. *Chem. Phys. Lett.* **1984**, *108*, 259. (d) Novoa, J. J.; Mota, F. *Chem. Phys. Lett.* **1985**, *119*, 135. (e) Heinrich, N.; Koch, W.; Frenking, G. *Chem. Phys. Lett.* **1986**, *124*, 20. (f) Galasso, V. *Chem. Phys.* **1989**, *138*, 231. (g) Guerra, M. *Chem. Phys. Lett.* **1990**, *167*, 315. (h) Falcetta, M.; Jordan, K. D. *J. Phys. Chem.* **1990**, *94*, 5666. (i) Chen, D.; Gallup, G. A. *J. Chem. Phys.* **1990**, *93*, 8893. (j) Chou, P. K.; Kass, S. R. *J. Am. Chem. Soc.* **1991**, *113*, 697.

(7) (a) Howard, A. E.; Staley, S. W. *A.C.S. Symp. Ser.* **1984**, *263*, 183. (b) Staley, S. W.; Strnad, J. T. Unpublished results.

(8) Kadifachi, S. *Chem. Phys. Lett.* **1984**, *108*, 233.

(9) Closs, G. L.; Krantz, K. D. *J. Org. Chem.* **1966**, *31*, 638.

(10) Cope, A. C.; Haven, A. C., Jr.; Ramp, F. L.; Trumbull, E. R. *J. Am. Chem. Soc.* **1952**, *74*, 4867.

(11) Lord, R. C.; Rea, D. G. *J. Am. Chem. Soc.* **1957**, *79*, 2401.

0022-3263/92/1957-0895$03.00/0

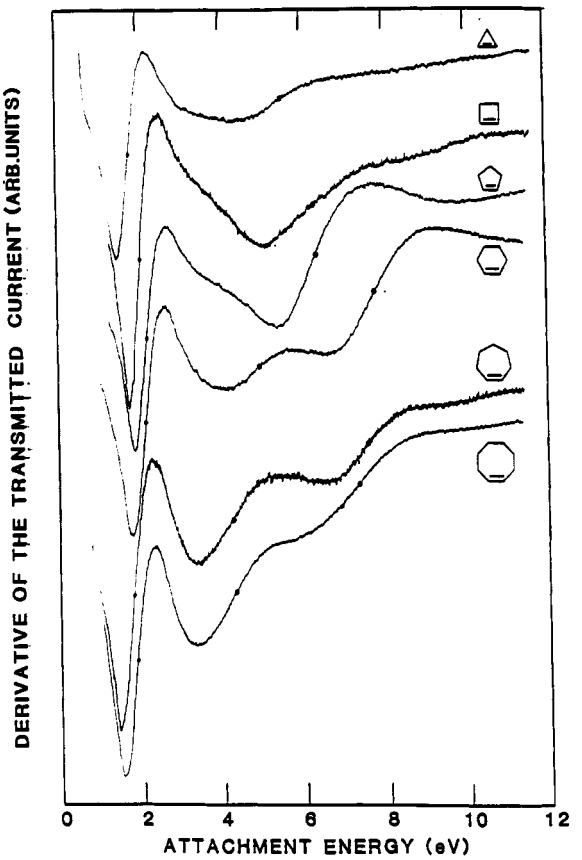

Figure 1. Electron transmission spectra of 3–8 obtained under high rejection conditions.

of the scattered electrons from reaching the collector. At energies that correspond to the attachment energies of the negative ion states, variations in the electron scattering cross-section can be seen. In order to accentuate these variations, a small (20–50 mV) AC voltage is applied to the collision chamber in order to obtain the derivative of the transmitted current with respect to energy. The $^2P_{3/2}$ resonance in argon was used to calibrate the spectra because of its narrow width, symmetrical profile, and relatively low energy.[12] The relative errors are estimated to be ±0.8% of the AE. The actual errors associated with these energies are probably much larger, on the order of ±0.05 eV at 2 eV. The uncertainty increases with the width of the resonance, which tends to be rather large, 3 eV or more above threshold.

We routinely collect ETS data under the extremes of both high and low rejection conditions.[13] High-rejection spectra (i.e., those that reflect the total electron scattering cross-section) are published in this study.

Molecular Orbital Calculations. Ab initio molecular orbital calculations employed the GAUSSIAN 90 series of programs[14] and the 6-31G[15a] and 6-31G*[15b] basis sets. The molecular structures for 1–8 used in this study are HF/6-31G-optimized geometries constrained to the following symmetries: C_{2v}, 1–4; C_s, 5 and 7; C_2, 6. No constraints were employed for the structure of 8.

Table I. Electron Attachment Energies of Ethylene, *cis*-2-Butene, and Cycloalkenes

compd	AE (eV) this work[a]	AE (eV) other results
1		1.74[b,c]
2		2.16,[b] 2.22[c]
3	1.73	
4	2.00	
5	2.14	2.13,[d] 2.26[e]
6	2.13	2.07,[f] 2.12,[e] 2.15[d]
7	1.79	1.82,[d] 1.97[e]
8	1.85	1.87,[e] 1.93[g]

[a] ±0.05 eV. [b] Reference 7a. [c] Reference 4c. [d] Reference 16. [e] Reference 8. [f] Reference 17. [g] Reference 18.

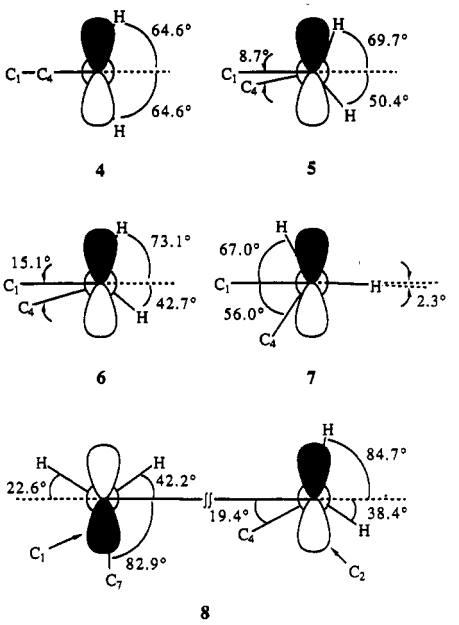

4 5 6 7 8

Figure 2. Newman projections and torsional angles for the allylic bonds of 4–8.

Analytical frequency analyses confirmed that all of these structures are true energy minima.

Results

Electron Transmission Spectroscopy. The ET spectra of 3–8 are shown in Figure 1. The attachment energies corresponding to the first resonances are listed in Table I. All of the spectra display a major (π^*) resonance near 2 eV, as well as one or more broad unassigned resonances above 4 eV.

Geometry-Optimized Structures. Optimized structures for 3–9 are given in Table II and Figure 2. Gas-phase structures have been determined for 3,[19] 4,[20] 5,[21] and 6[22] by microwave spectroscopy and for 5[23] and 7[24] by gas-phase electron diffraction. Ab initio geometry-optimized structures have been published for 3,[25] 4,[25] 5,[26] and 6[27] but only

(12) Read, F. H. *J. Phys. B.* **1968**, *1*, 893.
(13) Johnston, A. R.; Burrow, P. D. *J. Electron Spectrosc. Relat. Phenom.* **1982**, *25*, 119.
(14) Frisch, M. J.; Head-Gordon, M.; Trucks, G. W.; Foresman, J. B.; Schlegel, H. B.; Raghavachari, K.; Robb, M. A.; Binkley, J. S.; Gonzalez, C.; DeFrees, D. J.; Fox, D. J.; Whiteside, R. A.; Seeger, R.; Melius, C. F.; Baker, J.; Martin, R. L.; Kahn, L. R.; Stewart, J. J. P.; Topiol, S.; Pople, J. A. GAUSSIAN 90, Gaussian, Inc., Pittsburgh, PA, 1990.
(15) (a) Hehre, W. J.; Ditchfield, R.; Pople, J. A. *J. Chem. Phys.* **1972**, *56*, 2257. (b) Hariharan, P. C.; Pople, J. A. *Chem. Phys. Lett.* **1972**, *16*, 217. *Theor. Chim. Acta* **1973**, *28*, 213.
(16) Giordan, J. C. *Ph.D. Dissertation*, University of Maryland, 1980.
(17) Jordan, K. D.; Michejda, J. A.; Burrow, P. D. *Chem. Phys. Lett.* **1976**, *42*, 227.
(18) Allan, M.; Haselbach, E.; von Büren, M.; Hansen, H.-J. *Helv. Chim. Acta* **1982**, *65*, 2133.
(19) (a) Kasai, P. H.; Meyers, R. J.; Eggers, D. F., Jr.; Wiberg, K. B. *J. Chem. Phys.* **1959**, *30*, 512. (b) Stigliani, W. M.; Laurie, V. W.; Li, J. C. *J. Chem. Phys.* **1975**, *62*, 1890.
(20) Bak, B.; Led, J. J.; Nygaard, L.; Rastrup-Andersen, J.; Sørensen, G. O. *J. Mol. Struct.* **1969**, *3*, 369.
(21) Rathjens, G. W., Jr. *J. Chem. Phys.* **1962**, *36*, 2401.
(22) Scharpen, L. H.; Wollrab, J. E.; Ames, D. P. *J. Chem. Phys.* **1968**, *49*, 2368.
(23) (a) Chiang, J. F.; Bauer, S. H. *J. Am. Chem. Soc.* **1969**, *91*, 1898. (b) Geise, H. J.; Buys, H. R. *Rec. Trav. Chim.* **1970**, *89*, 1147.
(24) (a) White, D. N. J.; Bovill, M. J. *J. Chem. Soc., Perkin Trans. 2* **1977**, 1623. (b) Ermolaeva, L. I.; Mastryukov, V. S.; Allinger, N. L.; Almenningen, A. *J. Mol. Struct.* **1989**, *196*, 151.
(25) Wiberg, K. B.; Wendoloski, J. J. *J. Am. Chem. Soc.* **1982**, *104*, 5679.

Table II. Structural Parameters[a] of Geometry-Optimized Cycloalkenes and Related Compounds

compd	r(C=C)	r(C2C3)	r(C3C4)	r(C4C5)	r(C5C6)	∠(C=C—C)	α[b]	β[b]
1	1.3220							
2	1.3272	1.5029				128.14		
3	1.2864	1.5151				64.88		
4	1.3305	1.5243	1.5742			94.59		
5	1.3239	1.5118	1.5533			112.51	165.82	
6	1.3258	1.5089	1.5346	1.5335		123.68	28.88	
7	1.3259	1.5113	1.5391	1.5345		125.98	130.36	122.46
8	1.3273	1.5085	1.5354	1.5477	1.5379	130.30		
		1.5122	1.5468	1.5352		131.14		

[a] Bond lengths in Å; angles in deg; optimized at HF/6-31G. [b] Defined as in the following figures:

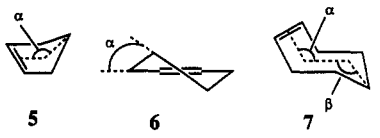

5 6 7

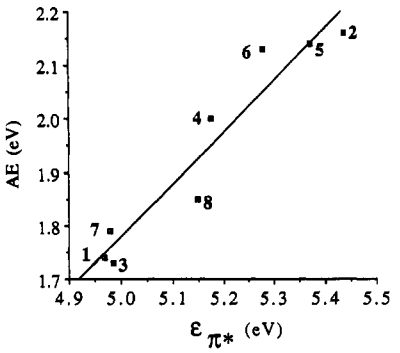

Figure 3. Plot of attachment energies versus π* orbital energies for 1–8. (The AEs for 1 and 2 are from ref 7a.)

Table III. π* Orbital Energies and π-Electron Densities for Cycloalkenes and Related Ethylenes[a]

compd	ε_π* (eV) alkene or cycloalkene	ε_π* (eV) ethylene[b]	ρ_π[c]
1	4.97	4.97	2.0000
2	5.44	4.94	2.0126
3	4.99	5.22	1.9254
4	5.18	4.91	1.9798
5	5.37	4.95	1.9972
6	5.28	4.95	2.0096
7	4.98	4.94	2.0107
8	5.15	4.94	2.0142

[a] Calculated at the HF/6-31G*//HF/6-31G level. [b] ϵ_{π^*} for ethylene with r(C=C) fixed at the values for 2–8. [c] In electrons; includes contributions of the $2p_y$, $3p_y$, d_{xy} and d_{yz} atomic orbitals.

semiempirical molecular orbital structures and molecular mechanics structures have been reported for 7[24] and 8.[28]

Discussion

Experimental Attachment Energies. The relative AE(π*) values that we have measured agree with those determined by other groups with one significant exception (Table I). Kadifachi has reported that the AEs of 5–8 decrease in a regular fashion so that AE of 7 is 0.1 eV greater than AE of 8.[8] In contrast, we have determined that AE of 7 is actually 0.06 eV *less* than AE of 8 and that a monotonic decrease does not exist on going from 5 to 8.

Two considerations lead us to conclude that our AE values are correct. First, AEs nearly identical to ours were obtained by other investigators in the cases of 7[16] and 8,[18] whereas Kadifachi's value for 7 is at least 0.15 eV larger. Second, π* orbital energies (ϵ_{π^*}) of 1–8 at the HF/6-31G*//HF/6-31G level indicate that AE of 7 should lie *below* that of 8 (Table III). As seen in Figure 3, there is a good correlation between AE(π*) and ϵ_{π^*}. Such a correlation assumes the validity of a relative form of Koopmans' approximation[5] (eq 1), in which the difference in AE

$$\Delta AE = k\Delta\epsilon_{\pi^*} \quad (1)$$

(ΔAE) is proportional to the difference in ϵ_{π^*} ($\Delta\epsilon_{\pi^*}$). We have shown that this correlation is optimal (correlation coefficient = 0.976) for 56 π* negative ion states of olefins, polyenes, benzene, and naphthalene at the HF/6-31G* level.[7b] Part of the scatter in this correlation is due to the uncertainties (up to ± 0.1 eV) in the experimental AE values. It is important to note that the use of diffuse functions seriously degrades the correlation owing to the fact that we are dealing with *unbound states*.

The correlation between AE(π*) and ϵ_{π^*} for 1–8 (Figure 3) has a slightly lower correlation coefficient (r = 0.961) than that for the series of compounds mentioned above. We note that the point for 8 is the one that lies farthest below the correlation line. Possible explanations are that 8 exists as a mixture of conformations or that the C_1 global minimum that we have calculated has a very shallow potential surface.[28] Molecular models suggest that the latter conformation is more flexible than the C_2 minimum for 6 or the C_s minimum for 7. In either case, the value of AE(π*) then would reflect electron scattering from a variety of conformations and might not correlate exactly with ϵ_{π^*} of the C_1 global minimum. Nevertheless, the fact that ϵ_{π^*} for the major conformation of 8 is calculated to be 0.17 eV greater than ϵ_{π^*} for 7 provides additional support for our relative AE values as opposed to those reported by Kadifachi.[8]

Structural Effects. Changes in ϵ_{π^*} arise from several different structural changes in these molecules. One obvious factor is the length of the double bond (r(C=C)), which ranges from 1.2864 Å in 3 to 1.3305 Å in 4 (Table II). The largest differences from the ethylene value occur in the small-ring compounds, primarily due to variations in the σ bond lengths of these compounds. Calculations of ethylene fixed at r(C=C) for 2–8 give values of ϵ_{π^*} that vary over a range of 0.31 eV (Table III).

Another structural change that is important in influencing ϵ_{π^*} is $\angle C_1C_2C_3$, which increases monotonically from 64.9° in 3 to 131.1° in 8. The effect of this change is to decrease the overlap integrals between the p_π atomic or-

(26) (a) Saebø, S.; Cordell, F. R.; Boggs, J. E. *J. Mol. Struct.* **1983**, *104*, 221. (b) Wiberg, K. B.; Bonneville, G.; Dempsey, R. *Isr. J. Chem.* **1983**, *23*, 85.
(27) Burke, L. A. *Theor. Chim. Acta* **1985**, *68*, 101.
(28) (a) Allinger, N. L.; Sprague, J. T. *J. Am. Chem. Soc.* **1972**, *94*, 5734. (b) Favini, G.; Rubino, C.; Todeschini, R. *J. Mol. Struct.* **1977**, *41*, 305 and references cited.

Table IV. Overlap Integrals for Cycloalkenes[a]

compd	$S(C_1C_3)$	$S(C_1H_3)$	$S(C_2H_3)$	$S(C_1H_{3'})$	$S(C_2H_{3'})$	$S(C_2H_{4'})$
4	0.264	0.059	−0.156	0.059	−0.156	
5	0.187	0.047	−0.183	0.031	−0.147	
6	0.152	0.043	−0.195	0.022	−0.137	0.094
7	0.145	0.060	−0.185	0.001	−0.008	0.171
8[b]	0.134	0.046	−0.201	0.011	−0.133	0.210
	0.135	0.039	−0.130	0.019	−0.082	0.155

[a] Corresponding to the orbital phases in Figure 8; H_3 and $H_{3'}$ refer to the upper and lower hydrogens, respectively, on C_3, etc. [b] The second line gives the values for $S(C_2C_8)$, $S(C_2H_8)$, $S(C_1H_8)$, $S(C_2H_{8'})$, $S(C_1H_{8'})$, and $S(C_1H_{8'})$, respectively.

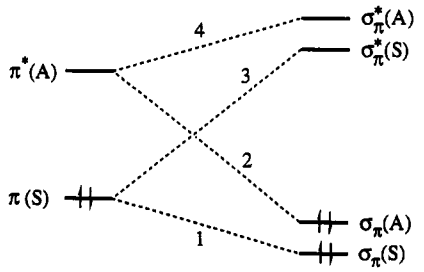

Figure 4. Interaction diagram for the mixing of π and π^* of ethylene with the pseudo-π CH_2 orbitals (σ_π and σ_π^*) of a cycloalkene ring.

bitals on C_1 and C_3 (Table IV). Finally, the $C_1C_2C_3C_4$ torsional angle increases from 0° in 4 to 8.7, 15.1, and 56.0° in 5, 6, and 7, respectively, at which point its average value decreases to 51.1° in 8 (Figure 2). These changes, coupled with a reduced distance between C_2 and the allylic (C_3) hydrogens with increasing ring size, cause significant changes in the overlap integrals between $C_1(p_\pi)$ and $C_2(p_\pi)$ and the alkyl orbitals (Table IV).

Influence of π-Electron Density. The major orbital interactions between the double bond and the alkyl fragment of a cycloalkene ring are illustrated in Figure 4. The π orbital (which is symmetric with respect to the molecular plane normal to the double bond in 3–7 and antisymmetric with respect to the C_2 axis in 6), can interact with the σ_π and σ_π^* orbitals of appropriate symmetry of the alkyl bridge (interactions 1 and 3, respectively), while the antisymmetric (C_s) or symmetric (C_2) π^* orbital can interact with the corresponding σ_π and σ_π^* orbitals (interactions 2 and 4, respectively). The energy of π^* is normally evaluated on the basis of only the latter two interactions. While interaction 1 undoubtedly has very little influence on ϵ_{π^*}, interaction 3 can have a significant influence.

Consider the series of compounds 1, 3, 9, and 10. The

9 10

lowest energy π^* orbital for each of these compounds is located *only* on the carbons of the ring double bond. Thus, interactions 2 and 4 in Figure 4 are zero because there are no antisymmetric π-type orbitals on C_3 in 3, 9, and 10 to interact with π^*. Nevertheless, ϵ_{π^*}(corrected) (ϵ_{π^*} corrected for the difference in ring double bond length relative to that of ethylene) varies *by nearly 1.5 eV* for this series of compounds. The origin of this dramatic effect is revealed by the excellent correlation ($r = 0.99$) in Figure 5 between ϵ_{π^*}(corrected) and the π-electron density in the ring double bond (ρ_π), which displays a slope of 5.38 eV/electron. (Although the ET spectroscopy of 10 has not been investigated, we have recently determined that the first resonance of 9 occurs at 0.86 eV,[29] in excellent agreement with

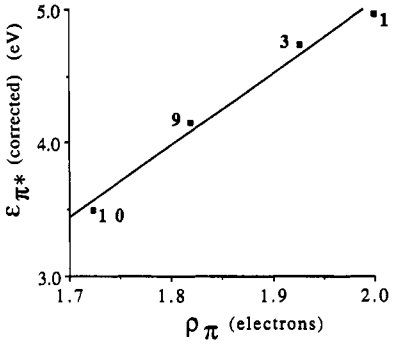

Figure 5. Plot of corrected HF/6-31G*//HF/6-31G π^* orbital energies (see text) versus π-electron densities for 1, 3, 9, and 10.

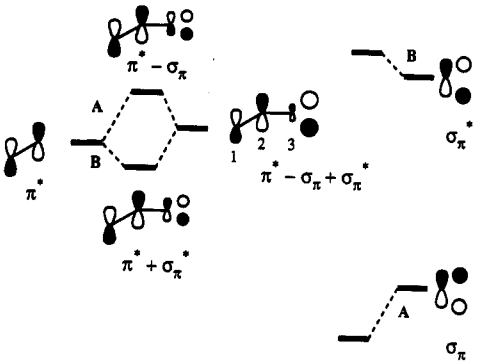

Figure 6. Interaction diagram for the mixing of the π^* component of propene with the pseudo-π methyl CH bonding (σ_π) and antibonding (σ_π^*) orbitals, with interaction energies of A and B, respectively.

the value predicted from the above-mentioned correlation of AE(π^*) with ϵ_{π^*}.[7b]) The increased importance of interaction 3 in Figure 4 on going from 3 to 10 causes a decrease in ρ_π that results in a decreased screening of π^* by the π electrons. This analysis supports our previous suggestion that 1 and 3 have nearly identical AE values owing to the compensating effects of a shorter double bond coupled with a decreased screening of π^* by π in 3 relative to 1.[7a]

The values of ρ_π calculated for the cycloalkenes are given in Table III. ρ_π increases by 0.089 electrons on going from 3 to 8, corresponding to a destabilizing influence on π^* of 0.48 eV. The origin of this effect is discussed in the next section.

Hyperconjugative Interactions of π^*. Hyperconjugation results from the mixing of a π or π^* orbital with a π-type bonding (σ_π) or antibonding (σ_π^*) orbital of an alkyl substituent, where σ_π mixes into π or π^* in an antibonding manner (A) while σ_π^* adds in a bonding manner (B) (Figure 6). Interaction A almost invariably predominates for π orbitals, whereas interactions A and B are more nearly balanced in the case of π^* orbitals.

According to second-order perturbation theory, the change in energy of π^* ($\Delta\epsilon_{\pi^*}$) that results from interaction

(29) Norden, T. D. *Ph.D. Dissertation*, University of Nebraska—Lincoln, 1987.

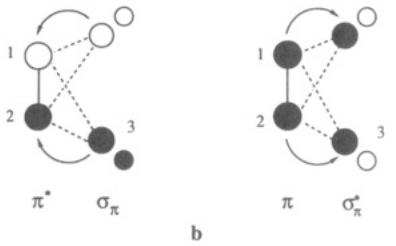

Figure 7. Interaction of the (a) π^* and (b) π orbitals of ethylene with the pseudo-π methylene antibonding (σ_π^*) and bonding (σ_π) orbitals, respectively, of appropriate symmetry to form *cis*-cycloalkenes **4**–**8**.

with a second orbital (e.g., σ_π^*) is given by eq 2, where π^* and σ_π^* are the unperturbed basis orbitals of energy ϵ_{π^*} and $\epsilon_{\sigma_\pi^*}$, respectively, and H is the interaction Hamiltonian.

$$\Delta\epsilon_{\pi^*} = \frac{\langle \pi^* | H | \sigma_\pi^* \rangle^2}{\epsilon_{\pi^*} - \epsilon_{\sigma_\pi^*}} \qquad (2)$$

Interaction A is small in propene because π^* and σ_π are very different in energy (i.e., the denominator of eq 2 is large). On the other hand, even though π^* and σ_π^* are much closer in energy, interaction B is about equally small. This results from the stabilizing interactions between C_2 and C_3 in $\pi^* + \sigma_\pi^*$ being partially cancelled by the longer range antibonding interactions between $C_2(p_\pi)$ and the methyl H(s) orbitals (i.e., the numerator of eq 2 is smaller for interaction B than for interaction A). Thus, although both the energy and the overlap terms in eq 2 are important, the latter will be shown to generally be the more important factor in understanding the AEs of **3**–**8**.

Consider interactions 2 and 3 in Figure 4 (i.e., the two electron interactions that lead to electron transfer). In interaction 2 ($\sigma_\pi \rightarrow \pi^*$; Figure 7a), the the antibonding overlap between C_1 and C_3 tends to partially cancel the bonding overlap between C_2 and C_3. As $\angle C_1C_2C_3$ is increased, the π overlap integral between C_1 and C_3 ($S_{C_1C_3}(3p_\pi - 3p_\pi)$) decreases (Table IV), whereas $S_{C_2C_3}(3p_\pi - 3p_\pi)$ varies only in the narrow range of 0.497–0.504 for **4**–**8**. (In Table IV we list the overlap integrals for only the diffuse $C(3p_\pi)$ and H(2s) orbitals, but the corresponding integrals for the $C(2p_\pi)$ and H(1s) orbitals show the same trends.) Thus, increasing $\angle C_1C_2C_3$ results in greater π-electron donation to the double bond via interaction 2.

In contrast, the C_1C_3 and C_2C_3 overlaps have the *same* sign in interaction 3 ($\pi \rightarrow \sigma_\pi^*$; Figure 7b) so that increasing $\angle C_1C_2C_3$ results in a *reduced* electron transfer out of the π bond. Thus, both of these interactions predict an increase in ρ_π on going from **3** to **8**. (A related analysis has been employed by Cessac and Bauld to explain the magnitude of ESR β hyperfine splittings (benzylic protons) of the ion radicals of benzocyclobutene and related compounds.[30]) A monotonic increase in ρ_π is indeed calculated for this series (Table III).

Inspection of Figure 6 shows that the $C_3(p_\pi)$ components of σ_π and σ_π^* have opposite signs in the final wavefunction ($\pi^* - \sigma_\pi^* + \sigma_\pi$) and therefore tend to cancel, whereas the H(s) components have the same sign and consequently reinforce each other. Consideration of $C_3(p_\pi)$ in $\pi^* - \sigma_\pi^* + \sigma_\pi$ should therefore give an indication of the relative contributions of σ_π and σ_π^* to the "π^*" orbitals of **4**–**8** (i.e., the wavefunctions where the p_π orbitals on C_1 and C_2 are oriented perpendicular to the plane containing the double bond carbons and the two adjacent carbons) (Figure 8).

(30) Cessac, J.; Bauld, N. L. *J. Am. Chem. Soc.* **1976**, *98*, 2712.
(31) Jorgensen, W. L. *QCPE* **1977**, *11*, 340.

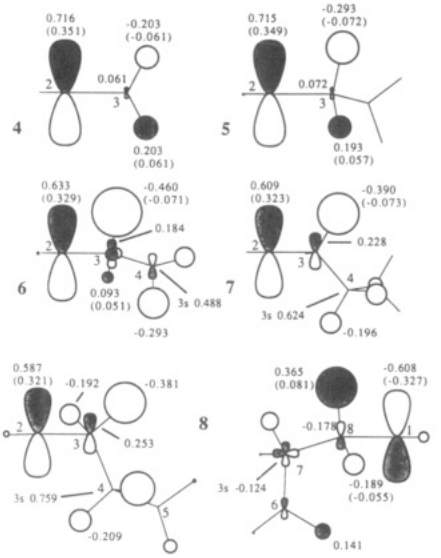

Figure 8. Views of the π^* orbitals of **4**–**8** along the CC axes of the double bonds with selected C(3s), C(3p), and H(2s) coefficients. (C(2p) and H(1s) coefficients >0.05 are given in parentheses.)

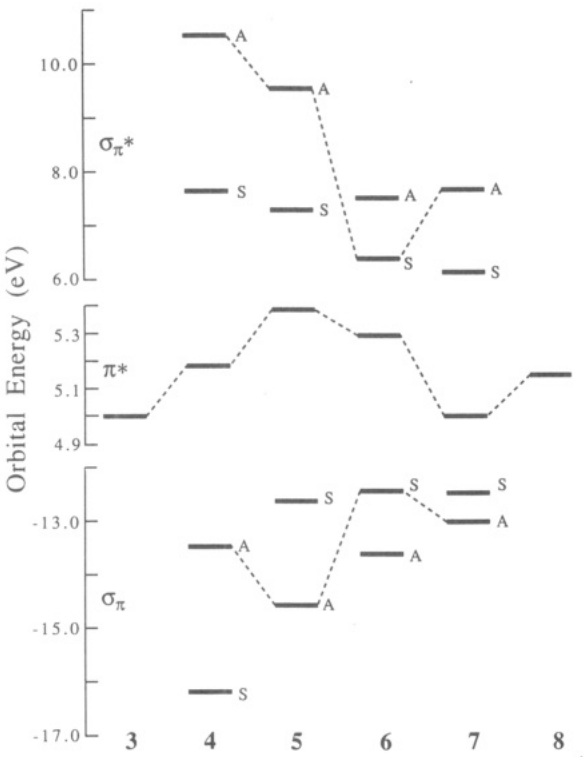

Figure 9. Energies of the π^* orbitals of **3**–**8** and of the pseudo-π and -π^* orbitals of the alkane fragments corresponding to **4**–**7**. The latter have the same geometries and orientations as the alkyl bridges in Figure 8 except that the allylic CC bonds have been replaced with CH bonds with optimized lengths. Correlation lines connect σ_π and σ_π^* orbitals that have the appropriate symmetry to interact with π^*.

The C(3s), $C(3p_\pi)$ and H(2s) orbital coefficients that are illustrated are the most sensitive to conformational changes in these compounds. Significant values for the energetically more important C(2p) and H(1s) coefficients found only at C_1 and C_2 and certain allylic hydrogens are given in parentheses.

The $C_2(3p_\pi)$ coefficient decreases from 0.715 to 0.633 while the $C_3(3p_\pi)$ coefficient increases from 0.072 to 0.184 on going from **5** to **6**. Clearly, there is a significantly larger contribution of σ_π^* to "π^*" in **6** than in **5**. This is due to two causes. First, the lowest σ_π^* orbital of appropriate

symmetry to mix with π^* does not interact as strongly in **5** as in **6** because the functions on C_4 of **5** lie near a nodal plane of π^*. Second, σ_π^* is lower in energy in **6** than in **5**.

The HF/6-31G*//HF/6-31G energies of the key σ_π^* basis orbitals in the alkyl bridges of **4–7** are illustrated in Figure 9. These were obtained by replacing $HC_1{=}C_2H$ of each cycloalkene (in the orientation shown in Figure 8) with two hydrogens at their optimized CH bond lengths. It can be seen that there is a large decrease in the energy of the lowest σ_π^* orbital that interacts with π^* (along with a smaller increase in the energy of the corresponding highest σ_π orbital) on going from **5** to **6**.

We believe that this decrease of σ_π^* plays the key role in keeping AE(π^*) of **6** equal to or below that of **5**. Indirect experimental support for this view can be seen in Figure 1. Note that in all of the ET spectra there are one or more "σ^*" resonances above 4 eV. We have not been able to assign specific orbitals or even symmetries to these resonances. (Indeed, some are broad enough that they may correspond to several overlapping resonances.) Nevertheless, it is interesting to note that AE for the first "σ^*" resonance decreases significantly on going from **5** to **6**.

The large decrease in energy of the σ_π^* orbitals that interact with π^* on going from **5** to **6** (Figure 9) is a consequence of the change in molecular symmetry from C_s to C_2. This can be shown by optimization of the C_s (boat) stationary point for **6**. The HF/6-31G*//HF/6-31G energy of the lowest antisymmetric σ_π^* orbital of the alkyl fragment increases from 6.35 eV for the C_2 (chair) form to 8.11 eV for the C_s (boat) form, primarily because of antibonding interactions across the eclipsed C_4C_5 bond in the latter that are not present in the former.

The increased contribution of σ_π^* to "π^*" on going from **6** to **7** is reflected in the decrease and increase, respectively, of the $C_2(p_\pi)$ and $C_3(p_\pi)$ coefficients (Figure 8). Since $\epsilon_{\sigma_\pi^*}$ for the alkyl fragment of **7** is greater than that for **6**, the decrease in ϵ_{π^*} *cannot* be caused by the energy term in eq 2. However, following eq 2, the sum of the squares of the overlap integrals between $C_2(3p_\pi)$ and H(2s) for the vicinal allylic hydrogens ($\sum S^2_{CH}$) change in almost the same order (**3** < **4** < **5** < **6** > **7** < **8**) as does ϵ_{π^*} (**3** < **4** < **5** > **6** > **7** < **8**).

The former order can be understood as follows. As shown in Figure 2, the $C_1C_2C_3C_4$ torsional angle increases on going from **4** to **7** and then decreases (on average) in **8**. An increase in this angle has the effect of rotating C_4 below the double bond so that the hydrogens on C_3 eventually overlap less with $C_2(p_\pi)$ whereas C_4 and its hydrogens overlap more. Since the former overlap is antibonding in "π^*" whereas the latter are antibonding and bonding, respectively (thereby reducing their net interaction) (Figure 8), *the effect of twisting about C_2C_3 will be to stabilize* "π^*", primarily by decreasing the antibonding overlap between π^* and σ_π^* at the allylic hydrogens.

The difference in the above orders on going from **5** to **6** is discussed in the next to last section. Model calculations on propene in the last section give further insight into how the torsional angle affects ϵ_{π^*}.

$\Delta\epsilon_{SCF}$ Calculations. A second approach to the theoretical analysis of AEs (other than Koopmans' theorem) is by calculation of the difference in total energy of the ground and negative ion states at the geometry of the former ($\Delta\epsilon_{SCF}$). This approach, while lacking the simple picture provided by a molecular orbital, is, in principle, more rigorous because it provides a difference in two *state energies* (Table V), which is the quantity that is being determined spectroscopically. The absence of vibrational structure in the π^* resonances in Figure 1 indicates that the resonances are short-lived enough for the assumption of negative ion states with geometries of the neutrals to be valid.

Table V. Total Energies and Differences in Total Energies for the Ground and Negative Ion States of 2–8

compd	total energy (h) ground state[a]	total energy (h) negative ion state[b]	$\Delta\epsilon_{SCF}$ (eV)
2	−156.107 804	−155.951 750	4.247
3	−115.822 389	−115.678 986	3.902
4	−154.899 326	−154.752 316	4.000
5	−193.977 068	−193.824 918	4.140
6	−233.019 557	−232.868 908	4.099
7	−272.045 915	−271.906 219	3.801
8	−311.069 424	−310.924 876	3.933

[a] RHF/6-31G*//HF/6-31G. [b] UHF/6-31G*//HF/6-31G.

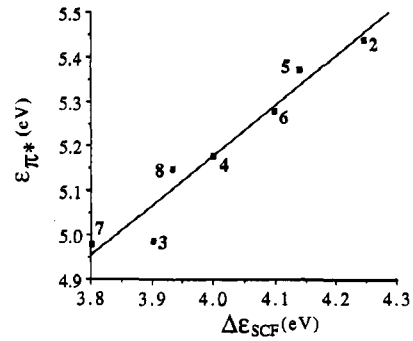

Figure 10. Plot of the RHF/6-31G* π^* orbital energies versus the differences in total energy of the ground and negative ion states (calculated at the RHF/6-31G* and UHF/6-31G* levels, respectively) of **2–8**.

A plot of ϵ_{π^*} against $\Delta\epsilon_{SCF}$ for **2–8** shows a good correlation (r = 0.97; Figure 10). However, comparison of the "π^*" wavefunctions of **2–8** with the changes in electron density on going from the ground states to the negative ion states ($\Delta\rho$) reveals significant differences. As illustrated for **7** in Figure 11a, "π^*" is located primarily on the $C_1(p_\pi)$ and $C_2(p_\pi)$ orbitals and on adjacent H(s) and C(s) orbitals that overlap with $C_1(p_\pi)$ and $C_2(p_\pi)$. In contrast, $\Delta\rho$ is positive not only for $C_1(p_\pi)$ and $C_2(p_\pi)$ but also at *all* of the hydrogens in **7**, whereas electron density is *lost* from the remaining C_1 and C_2 orbitals and from C_3–C_7 (Figure 11b). Analysis of the data for **2–8** further reveals that (a) for the two hydrogens on a given allylic carbon, $\Delta\rho$ is larger for the hydrogen with the larger H(2s) coefficient in Figure 8, but only by a small amount, (b) $\Delta\rho$ is larger (sometimes by a factor of 2 or more) on the more peripheral (or "equatorial") hydrogen of a nonallylic methylene group, and (c) $\Delta\rho$ is *always* largest for the olefinic hydrogens, even though they lie essentially in the nodal plane of the $C_1(p_\pi)$ and $C_2(p_\pi)$ orbitals.

Although the coefficients in "π^*" of **2–8** do not closely reflect $\Delta\rho$ in these compounds, there are apparently enough similarities in the two approaches (particularly with regard to the important allylic hydrogens) for the application of Koopmans' approximation to be valid to a high degree. However, the large 3s coefficients on C_4 of **6–8** (see Figure 11a) are *not reflected* in the corresponding changes in electron density for either this orbital or this carbon in the negative ion states.

Comparison of ϵ_{π^*} in Cycloalkenes 3–8. In this section we analyze the relative ϵ_{π^*} values of **3–8** with regard to the various effects discussed above. A semiquantitative summary of this analysis is given in Table VI. Here, the difference between ϵ_{π^*}(cycloalkene) and ϵ_{π^*}(ethylene) ($\Delta\epsilon_{\pi^*}$(total)) is broken down into three contributions. The

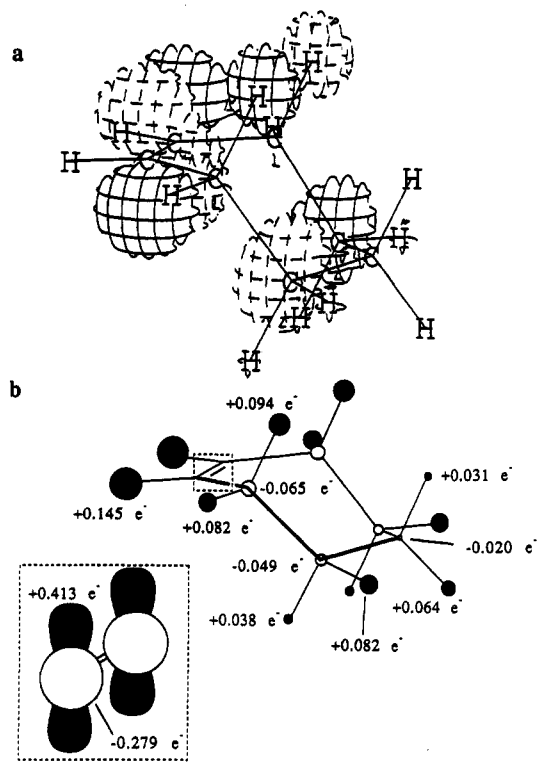

Figure 11. (a) Psi 77[31] drawing of the C(3s), C(3p), and H(2s) functions of the HF/6-31G* π^* orbital of cycloheptene; (b) drawing illustrating the changes in HF/6-31G* electron density on going from the ground state to the π^* negative ion state of cycloheptene. The inset shows a gain for C(p_π) and a loss for all of the other orbitals of C_1 and C_2.

Table VI. Differences in π^* Orbital Energies of Cycloalkenes Relative to Ethylene[a]

compd	$\Delta\epsilon_{\pi^*}(r(C{=}C))^b$	$\Delta\epsilon_{\pi^*}(\rho_\pi)^c$	$\Delta\epsilon_{\pi^*}$(other)^d	$\Delta\epsilon_{\pi^*}$(total)^e
3	+0.23	−0.40	+0.19	+0.02
4	−0.06	−0.11	+0.38	+0.21
5	−0.02	−0.02	+0.44	+0.40
6	−0.02	+0.05	+0.28	+0.31
7	−0.03	+0.06	−0.02	+0.01
8	−0.03	+0.08	+0.13	+0.18

[a] In eV; calculated at HF/6-31G*//HF/6-31G. [b] From column 3, Table III. [c] $\Delta\epsilon_{\pi^*}(\rho_\pi) = \Delta\rho_\pi$ (Table III, column 4) × 5.38 eV/electron. [d] $\Delta\epsilon_{\pi^*}$(other) = $\Delta\epsilon_{\pi^*}$(total) − $\Delta\epsilon_{\pi^*}(r(C{=}C))$ − $\Delta\epsilon_{\pi^*}(\rho_\pi)$. [e] From column 2, Table III.

term $\Delta\epsilon_{\pi^*}(r(C{=}C))$ is a correction for changes in the length of the double bond while $\Delta\epsilon_{\pi^*}(\rho_\pi)$ is a correction for π-electron density (both relative to ethylene). All other contributions are grouped under $\Delta\epsilon_{\pi^*}$(other).

The bond length and π-electron density corrections are approximately equal and opposite in **3**, as previously suggested.[7a] The bond length corrections in the other *cis*-cycloalkenes are quite small while the π-electron density corrections are somewhat larger, reaching −0.11 eV for **4** and spanning a range of 0.19 eV between **4** and **8**. This effect is surprisingly large and certainly was not suspected previously for the larger cycloalkenes.

The $\Delta\epsilon_{\pi^*}$(other) corrections have several components, but the single most important is $\sum S^2_{CH}$, which changes in the order **3** < **4** < **5** < **6** > **7** < **8**. This order is identical to the order for $\Delta\epsilon_{\pi^*}$(other) with the sole exception of the comparison of **5** and **6**. We therefore conclude that changes in CH overlaps (hyperconjugation) are primarily responsible for the significant range of $\Delta\epsilon_{\pi^*}$(other) contributions in Table V. These changes are a direct consequence of the various structural changes discussed above.

Finally, the difference in orders for $\sum S^2_{CH}$ and $\Delta\epsilon_{\pi^*}$(other) on going from **5** to **6** is undoubtedly influenced by the low value of $\epsilon_{\sigma_\pi^*}$ for the alkyl fragment of **6**. As discussed above, this decrease arises from the fact that the symmetry of the alkyl bridge changes from C_s in **5** to C_2 in **6**. A second factor which serves to decrease ϵ_{π^*} on going from **5** to **6** is the stabilizing overlap between $C_2(p_\pi)$ and $H_{4'}(s)$. Analogous overlaps are even more important in **7** and **8** (Table IV, last column).

Torsional Angle Dependence of ϵ_{π^*}. In order to more fully understand why ϵ_{π^*} is sensitive to the $C_1C_2C_3C_4$ torsional angle, we have optimized the geometries of various conformations of propene. ϵ_{π^*} is maximized (5.211 eV) in the staggered conformation ($\omega(HC_2C_3H)$ = 180°) and minimized (4.926 eV) in the less stable eclipsed (0°) conformation. (ϵ_π varies only 16% as much as ϵ_{π^*} and is at a minimum when the latter is at a maximum (and vice versa).)

The coefficients in "π^*" of propene clearly show a significant change in the mixing of π^* with σ_π^* on methyl rotation. Thus, those for $C_1(3p_\pi)$ and $C_2(3p_\pi)$ change from −0.729 and 0.729 to −0.685 and 0.654, respectively, on going from the staggered to the eclipsed conformation, whereas the methyl coefficients ($C_3(3p_\pi)$ and H(2s)) change from 0.064 and −0.274 to 0.278 and −0.461, respectively. This effect can only be due to a doubling of $S_{C_1H}(3p_\pi{-}2s)$ (from 0.031 to 0.060), since this is the only significant change in overlap that occurs on methyl rotation. The decrease in ϵ_{π^*} follows from the bonding overlap between ($C_1(3p_\pi)$ and H(2s) in π^* (Figure 6). Similar results are found for 1-butene.

These calculations and our ETS data thus lead to the general conclusion that *ϵ_{π^*} in alkenes is reduced by long-range overlap between C(p_π) and H(s) as the eclipsed conformation is approached.* This effect is much greater in the diffuse negative ion states than in the neutrals or radical cations.

Acknowledgment. We thank the National Science Foundation and the Pittsburgh Supercomputing Center for support and Professor Paul Burrow for his cooperation during the course of this research.

Registry No. 1, 74-85-1; 2, 590-18-1; 3, 2781-85-3; 4, 822-35-5; 5, 142-29-0; 6, 110-83-8; 7, 628-92-2; 8, 931-88-4.

Supplementary Material Available: Optimized geometries in the form of Z matrices, total and zero point energies, and dipole moments for 1–8 and 6(C_s) (8 pages). This material is contained in many libraries on microfiche, immediately follows this article in the microfilm version of the journal, and can be ordered from the ACS; see any current masthead page for ordering information.